

# Cortical neurons arise in symmetric and asymmetric division zones and migrate through specific phases

Stephen C Noctor<sup>1</sup>, Verónica Martínez-Cerdeño<sup>1</sup>, Lidija Ivic<sup>1</sup> & Arnold R Kriegstein<sup>1–3</sup>

Precise patterns of cell division and migration are crucial to transform the neuroepithelium of the embryonic forebrain into the adult cerebral cortex. Using time-lapse imaging of clonal cells in rat cortex over several generations, we show here that neurons are generated in two proliferative zones by distinct patterns of division. Neurons arise directly from radial glial cells in the ventricular zone (VZ) and indirectly from intermediate progenitor cells in the subventricular zone (SVZ). Furthermore, newborn neurons do not migrate directly to the cortex; instead, most exhibit four distinct phases of migration, including a phase of retrograde movement toward the ventricle before migration to the cortical plate. These findings provide a comprehensive and new view of the dynamics of cortical neurogenesis and migration.

The cerebral cortex is formed through the coordinated processes of neurogenesis and migration. Neurogenesis occurs within two proliferative regions of the embryonic cortical telencephalon. Cortical projection neurons are thought to be generated primarily in the VZ<sup>1</sup>, a pseudostratified neuroepithelial region that lines the lateral ventricles<sup>2</sup>, whereas some neurons<sup>3,4</sup> and postnatally generated glial cells arise in the SVZ<sup>5</sup>, a proliferative region that overlaps the basal VZ and extends into the intermediate zone (IZ). Neurogenesis occurs through a combination of several modes of cell division. These include symmetrical progenitor cell divisions that expand the pool of neuronal precursor cells, asymmetrical progenitor divisions that give rise to single neurons<sup>6,7</sup> and symmetrical terminal divisions, where a progenitor cell divides to produce two neurons, thus depleting the pool of proliferative cells<sup>7,8</sup>. It is generally thought that progenitor cells within the cortical VZ undergo all three of these modes of division.

Newly generated neurons reach the developing cortex either by somal translocation, whereby a neuron cell body travels within a pial contacting radial process<sup>9–11</sup>, or by locomotion, a process by which newborn neurons develop leading and trailing processes and migrate along radial glial fibers<sup>12</sup>. However, the dynamics of migration, as well as of neurogenesis, have not been directly observed in the context of the lineage relationship of individual cells. We examined the patterns of cell division and migration during late stages of neurogenesis by injecting a green fluorescent protein (GFP)-expressing retrovirus into the lateral ventricles of the developing rat cerebral cortex on embryonic day 16 (E16). These injections resulted in GFP labeling of progenitor cells and their clonal progeny. We prepared organotypic slice cultures 24 h after retroviral infections, and observed GFP<sup>+</sup> neural precursor cell divisions and migratory behavior in real time through confocal time-lapse microscopy. This approach allowed us to observe the dynamic behavior of clonally related families of cells. We found that radial glial cell divisions within the VZ produced postmitotic neurons

as well as intermediate precursor cells that migrated to the SVZ. Intermediate precursor cells divided symmetrically within the SVZ to produce pairs of neurons. Neuronal migration was characterized by distinct phases, which often included a phase of retrograde movement toward the ventricular surface before cells reversed direction and migrated to the cortical plate. We also observed individual radial glial cells that underwent multiple asymmetrical ‘self-renewing’ divisions, each yielding either a neuron or an intermediate precursor cell, before the same radial glial cell began to transform into an astrocyte.

## RESULTS

### Proliferation in the VZ

Our long-term time-lapse experiments allowed us to distinguish symmetrical from asymmetrical cell divisions. We adopted an operational definition to characterize the modes of cell division. We considered cell divisions to be symmetric if the morphology and behavior of the daughter cells were the same (*e.g.*, both neuronal or both progenitor) and asymmetric if the morphology and behavior of the daughter cells were different. Our studies therefore examined cell fate rather than potential. Using retroviral labeling and time-lapse imaging, we monitored the fates of 146 daughter cells generated by precursor cell divisions at E17–E19. Most, if not all, cortical progenitor cells in the VZ are radial glial cells<sup>13,14</sup>. We found that the majority of radial glial cell divisions (78.9%) resulted in an asymmetric fate for the daughter cells (Fig. 1e). These asymmetric divisions occurred at the ventricular edge and yielded two distinct daughter cells: a self-renewed radial glial cell, and a daughter cell that migrated away from the ventricle (Fig. 1a). We found that asymmetric divisions could be classified into three different subtypes. The majority, 65.8%, of the asymmetric divisions were neurogenic, whereas 7.3% could be described as asymmetric progenitor divisions, in that both the radial glial cell and the non-radial glial daughter cell re-entered the cell cycle and divided

Departments of <sup>1</sup>Neurology, <sup>2</sup>Pathology and the <sup>3</sup>Center for Neurobiology and Behavior, Columbia University College of Physicians & Surgeons, 630 W. 168<sup>th</sup> Street, New York, New York 10032, USA. Correspondence should be addressed to S.C.N. (scn8@columbia.edu).

Published online 4 January 2004; corrected 12 January 2004 (details online); doi:10.1038/nn1172

again. In the latter case, radial glial cell division produced a daughter cell that migrated away from the ventricle, rounded up, and divided in the SVZ (Fig. 1b,c). Finally, 26.9% of the asymmetric divisions were final radial glial divisions where the radial glial cell subsequently translocated away from the VZ.

A minority of radial glial divisions were symmetric progenitor divisions (9.6%, Fig. 1e and Supplementary Video 1 online) in which a radial glial cell divided to generate two radial glial cells that both remained in the VZ and subsequently divided. This type of division occurs frequently during early stages of cortical neurogenesis and less frequently at the end of neurogenesis<sup>8</sup> and is responsible for expanding the proliferative population. In 11.5% of radial glial divisions, we were not able to classify the mode of division.

### Proliferation in the SVZ

Asymmetrical progenitor divisions were identified when a daughter cell generated by radial glial cell division in the VZ subsequently moved to the adjacent SVZ and divided. We observed a total of 19 cell divisions within the SVZ. Cells generated in the VZ that then divided in the SVZ were termed intermediate progenitor cells. Of these SVZ divisions, 10.5% appeared to be symmetric progenitor divisions where both daughter cells divided again within the SVZ (Fig. 1f). However, the vast majority of SVZ divisions, 89.5%, appeared to be symmetric terminal divisions, producing two identical-looking cells that migrated toward the cortex (Fig. 1c).

### Migration

Very few daughter neurons simply migrated radially to the cortical plate after neurogenesis. Instead, the daughter cells exhibited four distinct phases of migration. During phase one, newborn neurons assumed a bipolar shape and ascended rapidly from the ventricular surface to the SVZ. During phase two, the daughter neurons stopped migrating, acquired a multipolar morphology, and remained in the SVZ for approximately 24 h (Fig. 1a,  $t = 36$  h). The majority of radial clones we observed in our time-lapse experiments (86.2%, 44/51) included at least one multipolar daughter cell in the SVZ at all times. Furthermore, we found that most (81.8%, 36/44) multipolar daughter cells showed dynamic behavior: they frequently changed orientation, and extended and retracted processes. After remaining in the SVZ for one day or more, a majority of the daughter cells (59.1%, 26/44) underwent a third phase of migration characterized by retrograde movement (Fig. 1a,  $t = 53$  h). The cells extended a leading process toward the ventricle, and the cell body moved closer to the ventricle. After contacting the ventricle, the daughter cells entered the fourth phase of migration. They reversed polarity, assumed the

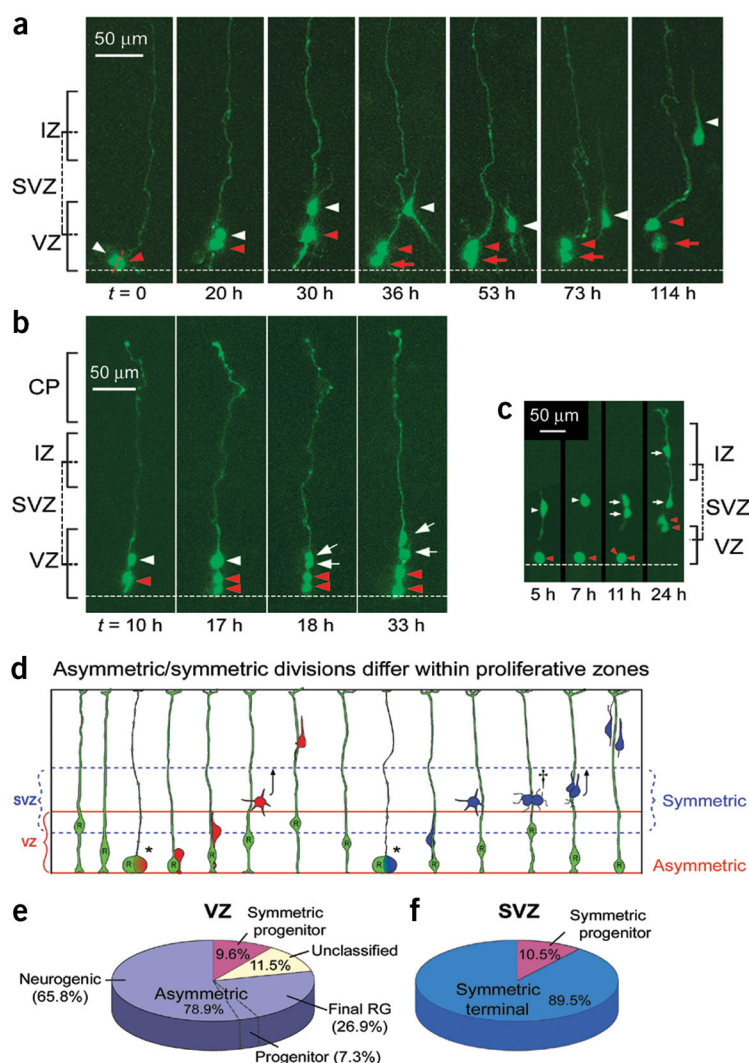


**Figure 1** Radial glial cells divide asymmetrically in the ventricular zone (VZ), and intermediate progenitor cells divide symmetrically in the subventricular zone (SVZ). **(a)** A radial glial cell (red arrowhead) divides asymmetrically at the ventricular surface to generate a daughter neuron (white arrowhead). The radial glial cell remains mitotic and generates another daughter cell (red arrow). **(b)** Radial glial cells also generate intermediate progenitor cells (white arrowhead) that divide symmetrically in the SVZ to generate two daughter cells (white arrows) that migrate toward the cortical plate (CP). **(c)** A further example of a symmetric neurogenic division within the SVZ followed by radial migration of the daughter cells (arrows). Note that the parental radial glial cell (arrowhead) underwent an additional mitosis prior to the 24 h frame. IZ, intermediate zone. **(d)** Scheme depicting separate niches for asymmetric and symmetric neurogenic divisions. Neurogenic radial glia (R) divide asymmetrically in the VZ (\*) to self-renew and generate neurons either directly (red cell) or indirectly through generation of an intermediate progenitor cell (blue). Terminal symmetric divisions occur in the SVZ (dagger). **(e)** At E17–19, the majority of radial glial cell divisions in the VZ are asymmetric. **(f)** Most divisions of intermediate progenitor cells in the SVZ produce two post-mitotic neurons (symmetric terminal), while a minority produce additional pairs of progenitor cells (symmetric progenitor).

bipolar morphology of a migrating neuron and recommenced migration toward the cortical plate (Fig. 1a,  $t = 73$ –114 h). Retrograde movement preceding migration to the cortical plate was also observed for symmetric cells generated in the SVZ. The rate of radial migration during the final phase was significantly slower ( $6.4 \pm 0.7 \mu\text{m/h}$ ,  $n = 10$ ) than during the first phase ( $19.7 \pm 6.2 \mu\text{m/h}$ ,  $n = 7$ ,  $P < 0.01$ ).

Some daughter cells in the SVZ (27.4%, 14/51) did not descend to the ventricle but nevertheless paused within the SVZ, and 9.8% (5/51) stayed there for the duration of the experiment. A minority of SVZ

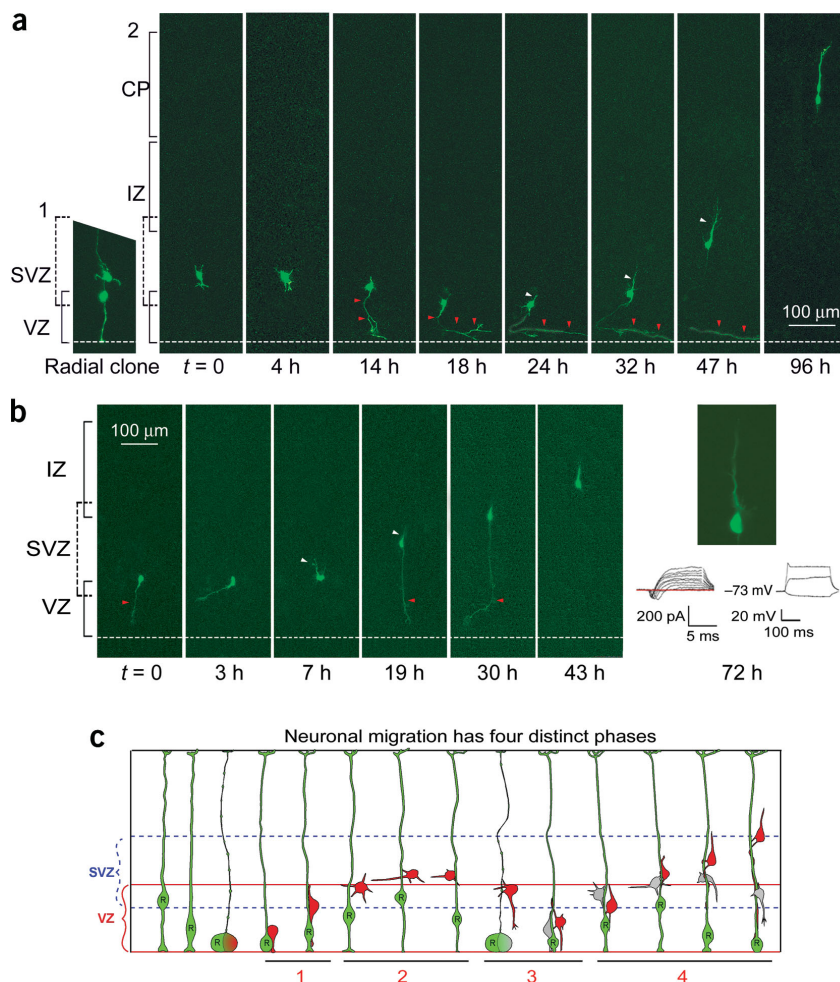


**Figure 2** Neocortical neurons exhibit four distinct phases of migration. **(a)** Left, phase one: the first phase after generation at the ventricular surface is a rapid radial migration to the subventricular zone (SVZ). The second phase (starting with tall panels) consists of migratory arrest for 24 h or more (shown here at the end of phase two,  $t = 0$  h), followed by a third phase of retrograde migration toward the ventricle ( $t = 4$ – $18$  h), and a final phase of polarity reversal and migration toward the cortical plate (CP;  $t = 24$ – $96$  h). These neurons often leave a trailing axon in the ventricular zone (VZ, red arrowheads). Also see **Supplementary Video 2** online. **(b)** A neuron shown during phase three ( $t = 0$ – $3$  h) and four ( $t > 7$  h) of migration. The right panel shows the appearance of the neuron and its electrophysiological membrane properties at 72 h. IZ, intermediate zone. **(c)** Scheme depicting a neuron (red) undergoing the four phases of migration: (1) initial radial migration, (2) SVZ arrest, (3) retrograde migration, and (4) secondary radial migration.

cells (7.8%, 4/51) subsequently resumed migration toward the cortical plate. It is possible that some of these cells made a ventricular approach, but the behavior occurred between the time-points when we imaged the slices. Alternatively, these cells may represent a subset of neocortical neurons that do not approach the ventricle before recommencing migration.

To further examine the migratory behavior of individual daughter cells, and to unequivocally visualize individual cell processes obscured by adjacent GFP<sup>+</sup> radial glial cells, we observed the migratory behavior of GFP<sup>+</sup> single and double cell clones. The retrovirus we used randomly inserts the GFP reporter gene into one of the daughter cells after division. Thus, if a daughter neuron incorporated the GFP reporter gene, the GFP<sup>+</sup> ‘clone’ would consist of a single cell. On the other hand, if an intermediate progenitor cell incorporated the GFP reporter gene, the clone would consist of two cells at the next cell

cycle. We therefore reasoned that we would find GFP<sup>+</sup> single and double cell clones one day after infection. We prepared organotypic slice cultures on E17, the day after injection of low-titer retrovirus ( $1 \times 10^4$  colony-forming units), and observed single and paired GFP<sup>+</sup> cells.

Careful observation of the migratory behavior of these single and double cell clones revealed key features of the migratory phases in greater detail than we had previously observed in the radial clones. Most of the cells were in phase two (stationary phase in the SVZ) at the start of the time-lapse sequence. The majority of single and double cell clones exhibited retrograde movement toward the ventricle (64.7%, 11/17 single cells; 57.7%, 15/26 pairs; **Figs. 2** and **3**; **Supplementary Videos 2** and **3** online). During phase three (retrograde movement toward the ventricle), both single and paired neurons extended thin processes toward the ventricular surface and maintained this contact for 10 h or more. The final phase of migration consisted of radial locomotion to the cortical plate, as the neurons reversed polarity by developing leading processes oriented towards the pia (**Figs. 2a,b** and **3**; white arrowheads). The cells then acquired a bipolar morphology with a short leading process (average length  $95.0 \pm 21.5 \mu\text{m}$ ,  $n = 9$ ) and migrated radially to the cortex. We noted that pairs of neurons generated through symmetric divisions in the SVZ progressed through the phases of migration in tandem and migrated in close proximity to the same region of the cortical plate. The two-cell clones we observed in our time-lapse studies may correspond to the two-cell clones that have been previously observed at postnatal ages following *in utero* retroviral labeling<sup>15,16</sup>. The symmetrically generated neurons extended and retracted processes during migration, and migrated significantly slower during phase

four than single neurons generated by asymmetric division in the VZ ( $4.1 \pm 0.6 \mu\text{m/h}$  versus  $6.4 \pm 0.7 \mu\text{m/h}$ ,  $n = 10$ ,  $P < 0.05$ ). Regardless of whether neurons were generated in the VZ or SVZ, the majority showed retrograde movement toward the ventricle before migrating to the cortical plate.

Interestingly, most cells in phase four of migration retained the ventricle-contacting process. Thus, what had originally been the leading process of a daughter neuron as it approached the ventricle (**Figs. 2a,b** and **3a–c**; red arrowheads) became the trailing process of the neuron after it reversed polarity. The new trailing process lengthened significantly by growing tangentially within the VZ (**Supplementary Video 4** online). These processes were morphologically identified as axons based on their thin uniform caliber and trajectory. Many cortical neurons thus possessed axon-like processes at the start of phase four, which they maintained within the VZ during

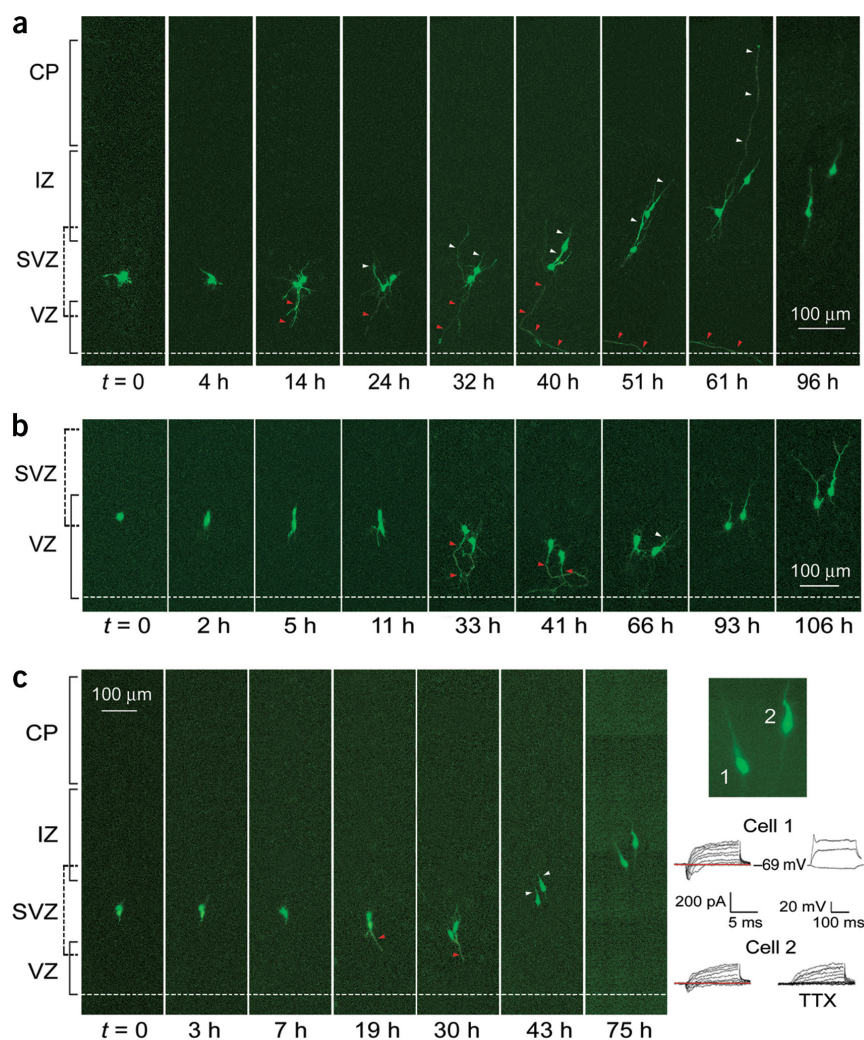


**Figure 3** Intermediate progenitor cells divide in the subventricular zone (SVZ) to generate pairs of neurons. **(a)** Double cell clones also undergo a phase of retrograde migration followed by migration to the cortex, and some leave trailing axons in the ventricular zone (VZ), red arrowheads). Leading processes can extend temporarily to reach the pia during migration (61 h, white arrowheads). **(b)** Another example of a progenitor cell undergoing symmetrical division in the SVZ to generate a pair of radially migrating neurons. Also see **Supplementary Video 3** online. **(c)** A pair of SVZ-generated cells recorded electrophysiologically after time-lapse imaging for 75 h. Both cells had membrane properties characteristic of young neurons including TTX-sensitive voltage-dependent inward  $\text{Na}^+$  current. IZ, intermediate zone; CP, cortical plate.

migration. These axons may ultimately reside in the white matter, as suggested by the finding that primate callosal neurons extend axons through the white matter during migration<sup>17</sup>. This mode of axonal outgrowth contrasts with that of cortical interneurons, which do not begin to develop axons until completing migration<sup>18–20</sup>.

### Identification of cell type

All single GFP<sup>+</sup> cells were located in the SVZ at the beginning of the time-lapse experiments. The majority of the single cells (70.8%, 17/24) developed morphological properties of neurons including neuritic and axonal processes and migrated radially to the cortex (**Fig. 2a,b**). We recorded electrophysiologically from ten single cells that had migrated to the cortical plate, and found that all had voltage-dependent currents characteristic of young neurons and were able to

generate small action potentials (**Fig. 2b**). A minority of the single cells (29.2%, 7/24) did not migrate, but divided in the SVZ. Most of these dividing cells ( $n = 5/7$ ) generated identical-looking daughter cells that developed neuronal morphology and migrated to the cortex (**Fig. 3**). In some cases, ( $n = 2$ ) we used patch-clamp recording to characterize whole-cell currents in GFP<sup>+</sup> cells following a sequence of time-lapse imaging. We found that the daughter cells generated in the SVZ that had subsequently migrated for three days in culture, had TTX-sensitive voltage-dependent inward currents characteristic of young neurons (**Fig. 3c**, cells 1 and 2). We also recorded electrophysiologically from GFP<sup>+</sup> pairs of cells identified in acute slices. Recordings demonstrated responses to the amino acid transmitters glycine and GABA, as well as voltage-dependent inward currents typical of neurons (**Fig. 5d**).

To further characterize the single and double cell clones, we used immunohistochemistry with cell type-specific markers. The results suggested that single-cell clones were neurons or intermediate progenitor cells. Neuronal markers and membrane properties were already expressed in some single-cell clones 24 h after infection. We found 9/25 (36%) were immunopositive for the neuronal marker TuJ1 (**Fig. 4b**) and 6/13 (46%) had membrane properties characteristic of immature neurons (**Fig. 4e**). Consistent with some single-cell clones representing intermediate progenitor cells, 5/22 expressed the progenitor cell marker nestin (**Fig. 4f**), and 7/26 expressed the neuronal progenitor marker Sox1 (**Fig. 4f**). We also examined cell pairs for expression of cell type-specific markers. Out of 27 paired cells immunostained with TuJ1, 8 pairs (29%) showed TuJ1 staining (**Fig. 5b**), and of the remaining pairs, one cell of each was negative and the other weakly positive. Since antibody penetration can be variable, it is possible that some of these pairs may nonetheless consist of two neurons. Pairs of cells generated by progenitor cell divisions in

the SVZ also showed remarkable similarity in morphology and migratory behavior, as observed in 26 time-lapse experiments (see **Supplementary Video 3** online).

GABAergic interneurons and glial precursor cells generated in the ventral telencephalon are known to migrate tangentially into dorsal regions of the developing cerebral cortex<sup>21–23</sup>. To help determine whether any of our GFP<sup>+</sup> single or double cell clones had originated in the ventral telencephalon, we counterstained GFP<sup>+</sup> cells with antibodies that specifically label GABAergic interneurons (GABA), and oligodendrocyte precursor cells (NG2 and Olig2) one day after retroviral infection on E16. These ages were chosen to coincide with the time that we started our time-lapse experiments. We found that none of the multipolar single cells ( $n = 0/24$ , **Fig. 4d**), and none of the paired cells ( $n = 0/37$  pairs, **Fig. 5c**) were GABA<sup>+</sup>. In addition, we

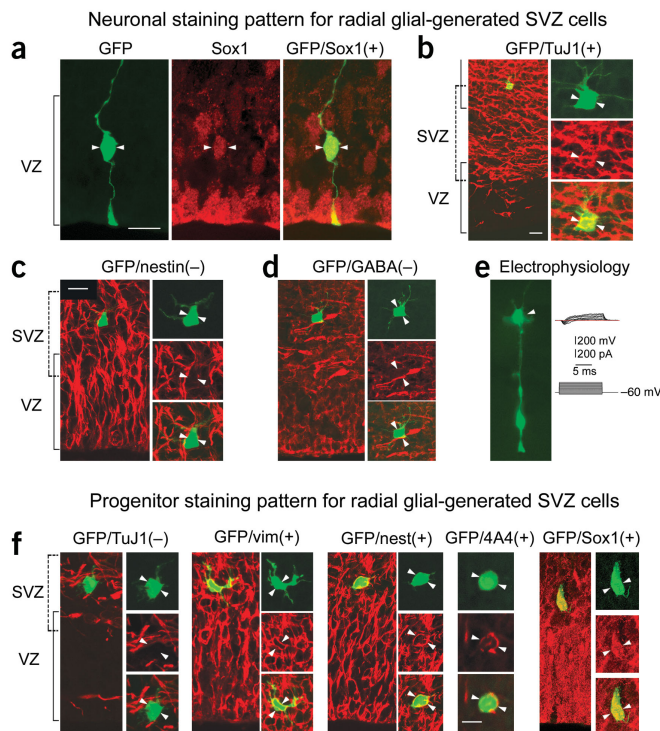


**Figure 4** Immunohistochemical and electrophysiological characterization of GFP<sup>+</sup> single-cell clones. **(a)** Neurogenic radial glial cells (green) are Sox1<sup>+</sup> and generate multipolar daughter neurons (green) that migrate to the SVZ and are TuJ1<sup>+</sup> **(b)**, but are nestin<sup>-</sup> **(c)** and GABA<sup>-</sup> **(d)**. **(e)** Daughter neurons in the SVZ have voltage-dependent currents characteristic of immature neurons. **(f)** Radial glia also generate intermediate progenitor cells that are TuJ1<sup>-</sup>, but stain positive for the progenitor cell markers vimentin (vim), nestin (nest), 4A4 and Sox1. Scale bars: **(a)** 10 μm, **(b)** 20 μm, **(c-f)** 10 μm.

of the parent radial glial cell and translocated over relatively long distances from the ventricular surface toward the cortical plate (21.2%, 11/52; Fig. 6a,b). In all cases, these divisions yielded two distinct daughter cells: one translocating cell (Fig. 6a,b, red arrowheads; Supplementary Video 5 online) and another multipolar daughter cell (Fig. 6a,b, red arrows). The daughter cells migrated slowly ( $4.1 \pm 0.8 \mu\text{m/h}$ ) away from the ventricle. When they reached the top of the VZ, both cells lost contact with the ventricular surface and began migrating more rapidly toward the cortical plate ( $8.9 \pm 2.8 \mu\text{m/h}$ ,  $P < 0.02$ ). In all cases, the multipolar daughter cells continued to migrate along with the translocating cells ( $n = 11/11$ ). The pial processes of the translocating cells maintained defining characteristics of radial glial fibers; they contacted blood vessels and had multiple branching endfeet at the pial surface (Fig. 6a).

We determined the phenotypes of translocating cells using patch-clamp recording and immunolabeling with neuronal and glial specific markers. Recordings obtained from translocating cells (Fig. 6b and 7g,  $n = 10$ ) demonstrated that they did not have the characteristic membrane properties of neurons and were physiologically indistinguishable from radial glial cells ( $n = 8$ ). Translocating cells had low membrane resistance ( $220.2 \pm 70.9 \text{ M}\Omega$ ) comparable to that obtained from radial glial cells ( $182.8 \pm 85.7 \text{ M}\Omega$ ,  $t$ -test  $P > 0.2$ ). In contrast, non-translocating daughter cells ( $n = 5$ ) had higher membrane resistance ( $1.2 \pm 0.5 \text{ G}\Omega$ ) and 2/5 had small inward voltage-gated currents characteristic of neurons. None of the translocating cells were TuJ1<sup>+</sup> ( $n = 0/11$ , Fig. 7a), but they were positive for the radial glial marker vimentin ( $n = 16/18$ , Fig. 7b), and were nestin<sup>+</sup> ( $n = 9/9$ , Fig. 7c). In addition, the majority of translocating cells ( $n = 24/25$ , Fig. 7d-f) expressed the astrocyte-specific marker GFAP, visible within the peri-nuclear cytoplasm. Thus, our data suggest that after a final asymmetric division, neurogenic radial glia translocate and transform into astrocytes.

We found that multipolar daughter cells generated at the final radial glial cell division behaved as intermediate progenitor cells. These cells migrated away from the ventricular surface, rounded up, and then divided in the SVZ, producing two morphologically identical daughter cells ( $n = 9$ , Fig. 6b). The resulting pair of cells then migrated to the cortex (Supplementary Video 5 online).

examined GABA expression in radial clones and found that none of the radially oriented migrating neurons were GABA<sup>+</sup>. Thus the single and paired neurons we observed in our time-lapse recordings were likely not tangentially migrating interneurons derived from the ventral telencephalon. We also immunostained tissue to determine the percentage of single GFP<sup>+</sup> cells that co-labeled with antibodies directed against oligodendrocyte precursor cells. We found that none of the GFP<sup>+</sup> cells were NG2<sup>+</sup> ( $n = 0/26$ ), but a small percentage (4.9%, 5/103) were Olig2<sup>+</sup>. However, these GFP<sup>+</sup>/Olig2<sup>+</sup> cells were small spherical cells found near the cortico-striatal junction and did not resemble the multipolar single-cell clones in the dorsal telencephalon that were imaged in our time-lapse studies. These results suggest that the single and double cell clones included in our analyses did not originate in the ventral telencephalon, but had been generated in the proliferative zones of the dorsal neocortex.

### Final radial glial divisions generate translocating cells

At the end stages of neurogenesis, we observed radial glial cells in the VZ undergoing divisions in which one daughter cell inherited the pial fiber

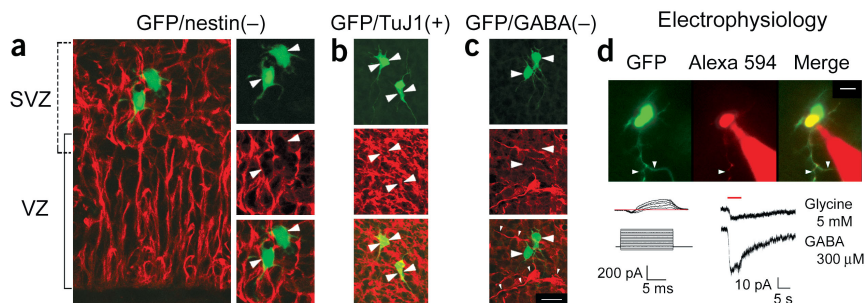


**Figure 5** Immunohistochemical and electrophysiological characterization of GFP<sup>+</sup> double cell clones. **(a)** Double cell clones (green) are nestin<sup>-</sup> and express neuronal markers including TuJ1 **(b)**. **(c)** Double cell clones are GABA<sup>-</sup>, whereas neighboring non-clonal tangential cells are GABA<sup>+</sup> (small arrowheads). **(d)** Double cell clones in the SVZ (green) demonstrate membrane properties characteristic of immature neurons (left trace), and respond to applications of the neurotransmitters GABA and glycine (in the presence of the GABA<sub>A</sub> receptor antagonist, bicuculline), as expected of young neurons (right traces). Red dye in the electrode (Alexa 594) confirmed recordings were from members of the GFP<sup>+</sup> clone. Scale bars: **(a)** 10 μm, **(b)** 20 μm, **(c,d)** 10 μm.

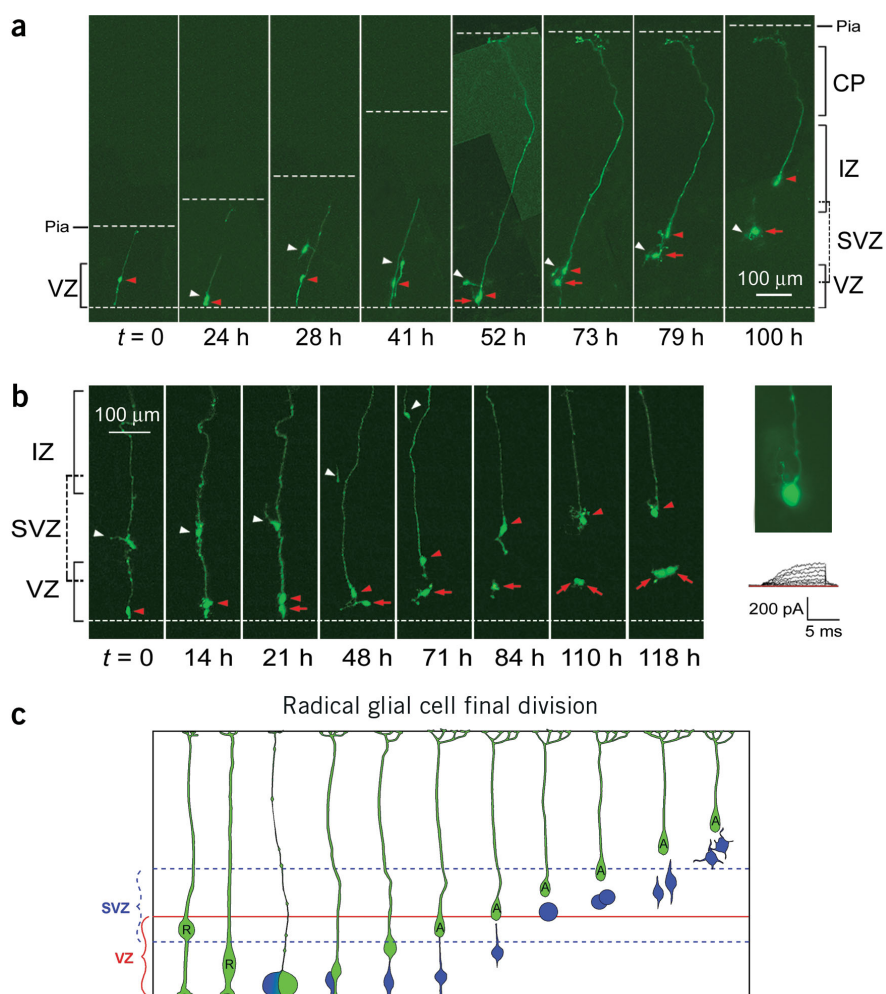


**Figure 6** Radial glial cells undergo final divisions to generate translocating radial glia and intermediate progenitor cells. **(a)** A radial glial cell (red arrowhead) divided asymmetrically in the VZ ( $t = 24$  h) to generate a presumed daughter neuron (white arrowhead) that underwent retrograde movement toward the ventricle ( $t = 41$ – $52$  h) before migrating toward the cortical plate ( $t = 73$ – $79$  h). Eventually the daughter cell moved deep into the tissue and out of range of laser detection ( $t = 100$  h). The radial glial cell divided a second time ( $t = 52$  h). One cell inherited the radial process and translocated toward the cortex (red arrowhead), while the other became multipolar (red arrow) and migrated to the SVZ. Also see **Supplementary Video 5** online. **(b)** Multipolar daughter cells (red arrow) are intermediate progenitor cells that subsequently undergo division ( $t = 110$  h) in the SVZ. This time lapse started on E18 and showed a radial glial cell translocate following division (arrowhead,  $t = 71$ – $118$  h). Electrophysiological recording from the translocating cell at 118 h demonstrated an absence of the voltage-dependent inward current found in young neurons. **(c)** Scheme summarizing the final division of radial glial cells (R) at the end of neurogenesis. After division, radial glial cells translocate and begin transformation into astrocytes (A). The newly generated daughter cells are intermediate progenitor cells (blue) that subsequently divide in the SVZ to generate two identical-looking cells.

## DISCUSSION

### Neuronal migration

Our findings indicate that many cortically derived neurons do not migrate directly to the cortical plate, but instead undergo four distinct phases of migration: phase one, rapid movement to the SVZ; phase two, migratory arrest in the SVZ; phase three, retrograde migration toward the ventricle; phase four, migration to the cortex. It has previously been suggested<sup>24</sup> that migrating neurons may pause or sojourn in the SVZ, and a recent report<sup>25</sup> demonstrates an abundance of migrating multipolar neurons in this embryonic region. By following the lineage of cor-

tical neurons, our data directly confirm that neurons born in the cortical VZ pause in the SVZ as multipolar neurons before resuming migration. The majority of neurons subsequently reverse polarity to move toward the ventricle. Interestingly, some striatally derived GABAergic interneurons destined for the cortex intercalate within the cortical VZ<sup>26</sup> and also migrate toward the ventricle before changing direction to migrate into the cortex<sup>27</sup>. Our observation of a similar phase of ventriculardirected movement during the migration of cortically derived pyramidal cells provides a potential convergence of the final phases of migration for these two major cortical cell types. The retrograde migration seen among neocortical-derived projection neurons could serve to coordinate their migration with that of ganglionic eminence-derived interneurons destined for the same radial column or cortical layer.

The four distinct phases of neuronal migration may have clinical significance in relation to neuronal migration disorders. In the human cortical malformation called ‘doublecortex,’ a band of cortical neurons fails to migrate fully into the cortex, and collects in the subcortical white matter<sup>28</sup>. It is possible that these neurons fail to migrate because they are not able to make the transition from phase two to phase three of migration and therefore remain as immature multipolar neurons in the subcortical white matter, as observed after RNA interference of doublecortin protein expression<sup>29</sup>. Similarly, periventricular nodular heterotopia, a condition in which neurons appear to be more mature than in double cortex but are found closer to the ventricle<sup>30</sup>, could represent a failure of neurons to initiate migration, but may alternatively reflect a failure to transit from phase three to phase four of migration. Specific gene defects are thought to interfere with the initiation, progression or termination of migration<sup>28</sup>. The present results suggest that some of these gene effects may be associated with the transition of neurons from one phase of migration to another.

Our results show that during late stages of rat neurogenesis, neurons do not inherit the pial fiber of the parent radial glial cell.

Instead they develop their own leading processes and migrate radially to the cortex. The cell that inherits the radial fiber at the final radial glial division translocates and appears to be a GFAP<sup>+</sup> glial cell. It has been established that radial glial cells translocate to the cortex as a first step in their transformation into astrocytes<sup>31,32</sup>, and we presume that the translocating cells we observed are transforming radial glia. Previous reports have suggested that many neurons may inherit the radial process of their parent radial glial cells and use somal translocation as a means of migration to the cortex<sup>9,10,33,34</sup>. However, it has been suggested that translocating neu-

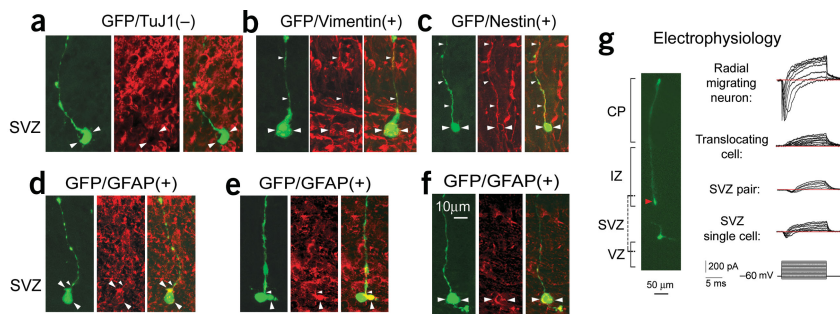


**Figure 7** Immunohistochemical and electrophysiological characterization of GFP<sup>+</sup> translocating cells indicates transformation into astrocytes. (a) Translocating GFP<sup>+</sup> (green) cells with soma in the SVZ are TuJ1<sup>-</sup>. (b) Translocating GFP<sup>+</sup> cells continue to express the radial glial marker, vimentin. (c) Translocating cells (green) are also positive for the proliferative cell marker, nestin. The cell fiber (small arrowheads) and soma (large arrowheads) are both nestin<sup>+</sup>. (d–f) Translocating GFP<sup>+</sup> cells express the astrocyte marker GFAP<sup>+</sup>, particularly in the proximal radial fibers (small arrowhead) and peri-nuclear cytoplasm (large arrowhead). (g) Whole-cell patch-clamp recordings help confirm cell identity. Radially migrating neurons show well-developed voltage-dependent inward currents (top trace). Translocating cells, in contrast, (left panel, red arrowhead) show lack of inward current (second trace from top). SVZ single and double cell clones show small voltage-dependent inward currents (bottom traces), consistent with neuronal identity.

rons are predominantly present at early stages of corticogenesis<sup>34</sup>. Our data are consistent with this scheme.

Previous studies using *in utero* retroviral labeling or transgenic mice have shown that while some clonally related cells in the postnatal neocortex are located in discrete clusters, other clones are widely dispersed<sup>15,16,35–40</sup>. The migration of GABAergic interneurons from the ganglionic eminence into the dorsal cortex may contribute partially to the tangential spread of clonal cells<sup>21,22</sup>, but this does not entirely account for the degree of wide dispersion that has been reported<sup>16,36,39</sup>. We observed that some daughter neurons migrated tangentially several cell-body lengths from their parental radial glial fiber during phase two, and others migrated tangentially from the parental fiber in phase four of migration. Thus, whereas some neurons migrate using parental radial glial fibers for guides<sup>41</sup>, other clonal neurons find alternate routes to the cortex, as previously suggested<sup>36,37</sup>.

## Neurogenesis

Our observations of asymmetric divisions within the VZ and symmetric divisions within the SVZ suggest that the VZ could be a niche for asymmetric neurogenic divisions, and the SVZ a niche for symmetric neurogenic divisions. This hypothesis is consistent with data concerning the distribution of the fate-determinant protein Numb. Both *in vitro* and *in vivo* genetic loss-of-function analyses have suggested that the asymmetric segregation of Numb is causal in determining cell identity in the nervous system<sup>42–44</sup>. In the mouse telencephalon, Numb is asymmetrically localized to the apical cytoplasm of mitotic VZ cells<sup>42</sup>. In most dividing cells of the SVZ, however, Numb is symmetrically distributed around the cell membrane<sup>45</sup>. This difference in Numb distribution within dividing cells of the VZ and SVZ supports the hypothesis that asymmetric divisions occur predominantly in the VZ, whereas symmetric divisions occur predominantly in the SVZ. Some dividing cells known to be present in the SVZ would not have been included in the present study. For example, cells generated in the VZ of the dorsal telencephalon at time points earlier than our infections would not have been included, and neither would proliferating cells generated in the ventral telencephalon that migrate tangentially into the cortical SVZ. Taken together, however, our data indicate that the SVZ is a niche for symmetric neurogenic divisions and a way station for neuronal migration.

The division patterns in the developing cortex and those described in the developing CNS of invertebrates are similar in certain respects. We have observed individual radial glial cells undergo asymmetric division to ‘self-renew’ and produce an intermediate progenitor cell that subsequently divides symmetrically to produce two neurons. This pattern of cell division resembles that of neuroblasts in *Drosophila melanogaster* CNS development, as these neuroblasts (analogous to radial glial cells) divide asymmetrically to self-renew and produce a ganglionic mother cell (GMC, analogous to the intermediate progenitor cell) that subsequently divides to produce two neurons or two glial cells<sup>46</sup>. However, unlike *D. melanogaster* neuroblasts, which undergo repeated asymmetric divisions, each producing a GMC, we have observed that successive radial glial cell divisions can produce single neurons and intermediate progenitor cells. Despite these differences, the similarities suggest that con-

served molecular mechanisms may underlie the patterns of progenitor cell divisions in the developing invertebrate CNS and the embryonic cerebral cortex.

Our data demonstrate the role of an intermediate progenitor cell, which undergoes symmetric neurogenic division within the SVZ, in the production of upper layer cortical neurons. This observation is consistent with the developmental expression pattern of the transcription factor Svet1. Svet1 appears first in proliferating SVZ cells and later in upper layer neurons, strongly suggesting that progenitor cells in the SVZ give rise to these neurons<sup>47</sup>. Indeed, it has been proposed that the SVZ may be the major source for cortical neurons in the macaque<sup>48</sup>. Of interest, during human cortical development, a subset of GABAergic interneurons is generated in the cortical SVZ<sup>4</sup>. The cells we have observed that are generated in the rodent SVZ may similarly include a population of cortically derived interneurons. Our data complement the Svet1 finding by showing that progenitor cells originating in the VZ move to the SVZ where they divide in the next cell cycle to produce progeny that then migrate into the cortex. Furthermore, the SVZ cell divisions appear to be symmetric, producing two neuronal progeny and depleting the precursor we term here an intermediate progenitor cell. The analogous role of the intermediate progenitor cell to that of the transit-amplifying cell observed during neurogenesis in the adult SVZ<sup>49</sup> and hippocampus<sup>50</sup> provides a link between the pattern of embryonic neurogenesis and the pattern of adult stem cell divisions.

## METHODS

**Animal surgery.** Replication-incompetent retrovirus ( $10^6$  c.f.u. or  $10^4$  c.f.u.) carrying the eGFP reporter gene was produced from the 293gp NIT-GFP retrovirus packaging cell line (generous gift from F. Gage, Salk Institute), and *in utero* injections into the lateral ventricles of rat embryos were performed as previously described<sup>41</sup>. All surgical procedures were performed in accordance with the Columbia University IACUC.

**Organotypic slice cultures.** Twenty-four hours after retroviral injections, embryos were killed and their brains removed and sectioned coronally as previously described<sup>41</sup>. Slices were transferred onto slice culture inserts (Millicell) in culture well plates (Gibco) with culture medium containing (by volume): 66% BME, 25% Hanks, 5% FBS, 1% N-2, 1% Pen/Strep/Glutamine (each from Gibco) and 0.66% d-(+)-glucose (Sigma).

**Confocal time-lapse imaging.** GFP<sup>+</sup> cells were imaged on an inverted Olympus Fluoview confocal microscope. Projection images were made from Z-stacks that included all visible processes of individual GFP<sup>+</sup> cells, and/or all visible GFP<sup>+</sup> cells within radial clones on a PC running Fluoview (Olympus). Transmitted light images were taken at each time point to track movements of the GFP<sup>+</sup> cells. Cell position was maintained relative to the ventricular surface until the cells had migrated out of the proliferative zones, after which the cell position was maintained relative to the pial surface for the duration of the time-lapse experiment. Between time points, slices were kept in a humidified incubator at 35 °C, 5% CO<sub>2</sub>. In some cases, cultured slices were transferred to an electrophysiological recording chamber for patch-clamp recording of GFP<sup>+</sup> cells. Montages were assembled, and time-lapse sequences arranged using Photoshop (Adobe Systems). We define the embryonic SVZ as a proliferative zone whose inferior border overlaps with the basal portion of the VZ and whose upper border extends into the lower region of the IZ. This definition conforms to the limits of the secondary proliferative population<sup>7</sup>.

**Electrophysiology.** Coronal slices for electrophysiological recordings of GFP<sup>+</sup> cells in E17–E22 rat neocortex were prepared as described previously<sup>41</sup>. Briefly, brains were embedded in 4% agar and sectioned at 400 μm with a vibratome (Leica) in ice-chilled artificial cerebrospinal fluid (ACSF) bubbled continuously with 95/5% O<sub>2</sub>/CO<sub>2</sub> containing 125 mM NaCl, 5 mM KCl, 1.25 mM NaH<sub>2</sub>PO<sub>4</sub>, 1 mM MgSO<sub>4</sub>, 2 mM CaCl<sub>2</sub>, 25 mM NaHCO<sub>3</sub> and 20 mM glucose; pH 7.4, at 25 °C, 310 mosm/l. Acute or cultured slices were transferred to a recording chamber on an Olympus BX50WI upright microscope and were perfused with aerated ACSF. GFP<sup>+</sup> cells were identified under epifluorescence and recordings performed using an EPC-9 patch-clamp amplifier (Heka Electronics) controlled by an Apple computer running Pulse v8.0 (Heka). Glass recording electrodes (5–7 MΩ) were filled with 130 mM KCl, 5 mM NaCl, 0.4 mM CaCl<sub>2</sub>, 1 mM MgCl<sub>2</sub>, 10 mM HEPES (pH 7.3) and 1.1 mM EGTA, to which 500 μM Alexa 594-conjugated biocytin (Molecular Probes) was added to identify recorded cells. Epifluorescent images of the recorded cells were collected using Scion Image, and arranged using Photoshop. Electrophysiological responses were measured and analyzed using Pulse (Heka), and traces were arranged using Igor Pro (Wavemetrics) and Freehand (Macromedia).

**Immunohistochemistry.** Rats (E17–E22) were perfused transcardially with ice-chilled saline, followed by 4% paraformaldehyde (PFA) in 0.1 M PBS, pH 7.4. Brains were post-fixed in PFA overnight, and sectioned on a vibratome (Ted Pella). After time-lapse imaging, selected slices were fixed by immersion in PFA. Slices were blocked at room temperature for 1 h with 10% serum, 0.1% triton X-100 and 0.2% gelatin in PBS. Antibodies were applied overnight at the following concentrations: TuJ1 polyclonal (Babco, 1:300), 4A4 monoclonal, (MBL International, 1:1,000), GFAP monoclonal (Sigma, 1:40), GABA monoclonal (Sigma, 1:1,000), vimentin monoclonal (Sigma, 1:40), nestin monoclonal (Chemicon, 1:40), Sox1 polyclonal (Chemicon, 1:250), NG2 polyclonal (Chemicon, 1:400), and Olig2 polyclonal (kind gift from T. Jessell and B. Novitch, Columbia University; 1:5,000). Sections were rinsed 3 × 10 min in PBS and secondary antibodies were applied at room temperature for 1 h. Secondary antibodies included Cy5-conjugated goat anti-mouse (Jackson ImmunoResearch; 1:50) and anti-rabbit (Jackson ImmunoResearch; 1:200). Secondary antibody for Sox1 was Texas red conjugated rabbit anti-chicken (Chemicon, 1:200). Sections were rinsed 3 × 10 min in PBS, and coverslipped with Aquamount (Lerner) before imaging.

**Confocal imaging.** Sections were imaged on an inverted Olympus Fluoview laser-scanning confocal microscope. Excitation/emission wavelengths were 488/515 nm (GFP), 568/590 nm (Texas red) and 685/690 nm (Cy5). Z-series images were collected at 1-μm steps in Fluoview (Olympus). To demonstrate co-labeling of GFP and cellular markers, only Z sections in the same focal plane as the GFP<sup>+</sup> cell bodies were used for analysis and for producing figures. Images were contrast-enhanced, assembled into montages, and false color was applied using Photoshop (Adobe).

*Note: Supplementary information is available on the Nature Neuroscience website.*

#### ACKNOWLEDGMENTS

We thank J. Goldman and members of the Kriegstein Lab for helpful comments on the manuscript, and W. Wong and J. Mirjahangir for technical assistance. This work was supported by National Institutes of Health grants (NS21223, NS38658 and NS35710) to A.R.K.

#### COMPETING INTERESTS STATEMENT

The authors declare that they have no competing financial interests.

Received 6 September; accepted 1 December 2003

Published online at <http://www.nature.com/natureneuroscience/>

- Parnavelas, J.G. The origin and migration of cortical neurones: new vistas. *Trends Neurosci.* **23**, 126–131 (2000).
- Boulder Committee. Embryonic vertebrate central nervous system: revised terminology. *Anat. Rec.* **166**, 257–261 (1970).
- Luskin, M.B. Restricted proliferation and migration of postnatally generated neurons derived from the forebrain subventricular zone. *Neuron* **11**, 173–189 (1993).
- Letinic, K., Zoncu, R. & Rakic, P. Origin of GABAergic neurons in the human neocortex. *Nature* **417**, 645–649 (2002).
- Privat, A. Postnatal gliogenesis in the mammalian brain. *Int. Rev. Cytol.* **40**, 281–323 (1975).
- Chenn, A. & McConnell, S.K. Cleavage orientation and the asymmetric inheritance of Notch1 immunoreactivity in mammalian neurogenesis. *Cell* **82**, 631–641 (1995).
- Takahashi, T., Nowakowski, R.S. & Caviness, V.S. The leaving or Q fraction of the murine cerebral proliferative epithelium: a general model of neocortical neurogenesis. *J. Neurosci.* **16**, 6183–6196 (1996).
- Cai, L., Hayes, N.L., Takahashi, T., Caviness, V.S., Jr. & Nowakowski, R.S. Size distribution of retrovirally marked lineages matches prediction from population measurements of cell cycle behavior. *J. Neurosci. Res.* **69**, 731–744 (2002).
- Morest, D.K. A study of neurogenesis in the forebrain of opossum pouch young. *Zeitschrift für Anatomie und Entwicklungsgeschichte* **130**, 265–305 (1970).
- Miyata, T., Kawaguchi, A., Okano, H. & Ogawa, M. Asymmetric inheritance of radial glial fibers by cortical neurons. *Neuron* **31**, 727–741 (2001).
- Nadarajah, B., Brunstrom, J.E., Grutzendler, J., Wong, R.O. & Pearlman, A.L. Two modes of radial migration in early development of the cerebral cortex. *Nat. Neurosci.* **4**, 143–150 (2001).
- Rakic, P. Neurons in rhesus monkey visual cortex: systematic relation between time of origin and eventual disposition. *Science* **183**, 425–427 (1974).
- Noctor, S.C. *et al.* Dividing precursor cells of the embryonic cortical ventricular zone have morphological and molecular characteristics of radial glia. *J. Neurosci.* **22**, 3161–3173 (2002).
- Hartfuss, E., Galli, R., Heins, N. & Gotz, M. Characterization of CNS Precursor Subtypes and Radial Glia. *Dev. Biol.* **229**, 15–30 (2001).
- Mione, M.C., Danevic, C., Boardman, P., Harris, B. & Parnavelas, J.G. Lineage analysis reveals neurotransmitter (GABA or glutamate) but not calcium-binding protein homogeneity in clonally related cortical neurons. *J. Neurosci.* **14**, 107–123 (1994).
- Reid, C.B., Tavazoie, S.F. & Walsh, C.A. Clonal dispersion and evidence for asymmetric cell division in ferret cortex. *Development* **124**, 2441–2450 (1997).
- Schwartz, M.L., Rakic, P. & Goldman-Rakic, P.S. Early phenotype expression of cortical neurons: evidence that a subclass of migrating neurons have callosal axons. *Proc. Natl. Acad. Sci. USA* **88**, 1354–1358 (1991).
- Parnavelas, J.G. & Lieberman, A.R. An ultrastructural study of the maturation of neuronal somata in the visual cortex of the rat. *Anat. Embryol. (Berl.)* **157**, 311–328 (1979).
- Shoukimas, G.M. & Hinds, J.W. The development of the cerebral cortex in the embryonic mouse: an electron microscopic serial section analysis. *J. Comp. Neurol.* **179**, 795–830 (1978).
- Miller, M.W. Maturation of rat visual cortex. III. Postnatal morphogenesis and synaptogenesis of local circuit neurons. *Brain Res.* **390**, 271–285 (1986).
- Anderson, S.A., Eisenstat, D.D., Shi, L. & Rubenstein, J. Interneuron migration from basal forebrain to neocortex: dependence on dlx genes. *Science* **278**, 474–476 (1997).
- de Carlos, J.A., Lopez-Mascaraque, L. & Valverde, F. Dynamics of cell migration from the lateral ganglionic eminence in the rat. *J. Neurosci.* **16**, 6146–6156 (1996).
- Novitsch, B.G., Chen, A.I. & Jessell, T.M. Coordinate regulation of motor neuron subtype identity and pan-neuronal properties by the bHLH repressor Olig2. *Neuron* **31**, 773–789 (2001).
- Bayer, S.A. & Altman, J. *Neocortical Development* (Raven Press, New York, 1991).
- Tabata, H. & Nakajima, K. Multipolar migration: the third mode of radial neuronal migration in the developing cerebral cortex. *J. Neurosci.* **23**, 9996–10001 (2003).
- Wichterle, H., Turnbull, D.H., Nery, S., Fishell, G. & Alvarez-Buylla, A. *In utero* fate mapping reveals distinct migratory pathways and fates of neurons born in the mammalian basal forebrain. *Development* **128**, 3759–3771 (2001).
- Nadarajah, B., Alifragis, P., Wong, R.O. & Parnavelas, J.G. Ventricle-directed migration in the developing cerebral cortex. *Nat. Neurosci.* **5**, 218–224 (2002).
- Gleeson, J.G. & Walsh, C.A. Neuronal migration disorders: from genetic diseases to developmental mechanisms. *Trends Neurosci.* **23**, 352–359 (2000).



29. Bai, J. *et al.* RNAi reveals doublecortin is required for radial migration in rat neocortex. *Nat. Neurosci.* **6**, 1277–1283 (2003).
30. Kakita, A. *et al.* Bilateral periventricular nodular heterotopia due to filamin 1 gene mutation: widespread glomeruloid microvascular anomaly and dysplastic cytoarchitecture in the cerebral cortex. *Acta Neuropathol. (Berl.)* **104**, 649–657 (2002).
31. Schmechel, D.E. & Rakic, P. A Golgi study of radial glial cells in developing monkey telencephalon: morphogenesis and transformation into astrocytes. *Anat. Embryol.* **156**, 115–152 (1979).
32. Voigt, T. Development of glial cells in the cerebral wall of ferrets: direct tracing of their transformation from radial glia into astrocytes. *J. Comp. Neurol.* **289**, 74–88 (1989).
33. Berry, M. & Rogers, A.W. The migration of neuroblasts in the developing cerebral cortex. *J. Anat.* **99**, 691–709 (1965).
34. Nadarajah, B. & Parnavelas, J.G. Modes of neuronal migration in the developing cerebral cortex. *Nat. Rev. Neurosci.* **3**, 423–432 (2002).
35. Parnavelas, J.G., Barfield, J.A., Franke, E. & Luskin, M.B. Separate progenitor cells give rise to pyramidal and nonpyramidal neurons in the rat telencephalon. *Cereb. Cortex* **1**, 463–468 (1991).
36. Walsh, C. & Cepko, C.L. Widespread dispersion of neuronal clones across functional regions of the cerebral cortex. *Science* **255**, 434–440 (1992).
37. O'Rourke, N.A., Dailey, M.E., Smith, S.J. & McConnell, S.K. Diverse migratory pathways in the developing cerebral cortex. *Science* **258**, 299–302 (1992).
38. Tan, S.S. & Breen, S. Radial mosaicism and tangential cell dispersion both contribute to mouse neocortical development. *Nature* **362**, 638–640 (1993).
39. Reid, C.B., Liang, I. & Walsh, C. Systematic widespread clonal organization in cerebral cortex. *Neuron* **15**, 299–310 (1995).
40. Kornack, D.R. & Rakic, P. Radial and horizontal deployment of clonally related cells in the primate neocortex: relationship to distinct mitotic lineages. *Neuron* **15**, 311–321 (1995).
41. Noctor, S.C., Flint, A.C., Weissman, T.A., Dammerman, R.S. & Kriegstein, A.R. Neurons derived from radial glial cells establish radial units in neocortex. *Nature* **409**, 714–720 (2001).
42. Zhong, W., Jiang, M.M., Weinmaster, G., Jan, L.Y. & Jan, Y.N. Differential expression of mammalian Numb, Numlike and Notch1 suggests distinct roles during mouse cortical neurogenesis. *Development* **124**, 1887–1897 (1997).
43. Cayouette, M. & Raff, M. Asymmetric segregation of Numb: a mechanism for neural specification from *Drosophila* to mammals. *Nat. Neurosci.* **5**, 1265–1269 (2002).
44. Shen, Q., Zhong, W., Jan, Y.N. & Temple, S. Asymmetric Numb distribution is critical for asymmetric cell division of mouse cerebral cortical stem cells and neuroblasts. *Development* **129**, 4843–4853 (2002).
45. Zhong, W., Feder, J.N., Jiang, M.M., Jan, L.Y. & Jan, Y.N. Asymmetric localization of a mammalian numb homolog during mouse cortical neurogenesis. *Neuron* **17**, 43–53 (1996).
46. Spana, E.P. & Doe, C.Q. The prospero transcription factor is asymmetrically localized to the cell cortex during neuroblast mitosis in *Drosophila*. *Development* **121**, 3187–3195 (1995).
47. Tarabykin, V., Stoykova, A., Usman, N., Gruss, P. Cortical upper layer neurons derive from the subventricular zone as indicated by Svet1 gene expression. *Development* **128**, 1983–1993 (2001).
48. Smart, I.H., Dehay, C., Giroud, P., Berland, M. & Kennedy, H. Unique morphological features of the proliferative zones and postmitotic compartments of the neural epithelium giving rise to striate and extrastriate cortex in the monkey. *Cereb. Cortex* **12**, 37–53 (2002).
49. Doetsch, F., Caillé, I., Lim, D.A., García-Verdugo, J.M. & Alvarez-Buylla, A. Subventricular zone astrocytes are neural stem cells in the adult mammalian brain. *Cell* **97**, 703–716 (1999).
50. Seri, B., García-Verdugo, J.M., McEwen, B.S. & Alvarez-Buylla, A. Astrocytes give rise to new neurons in the adult mammalian hippocampus. *J. Neurosci.* **21**, 7153–7160 (2001).